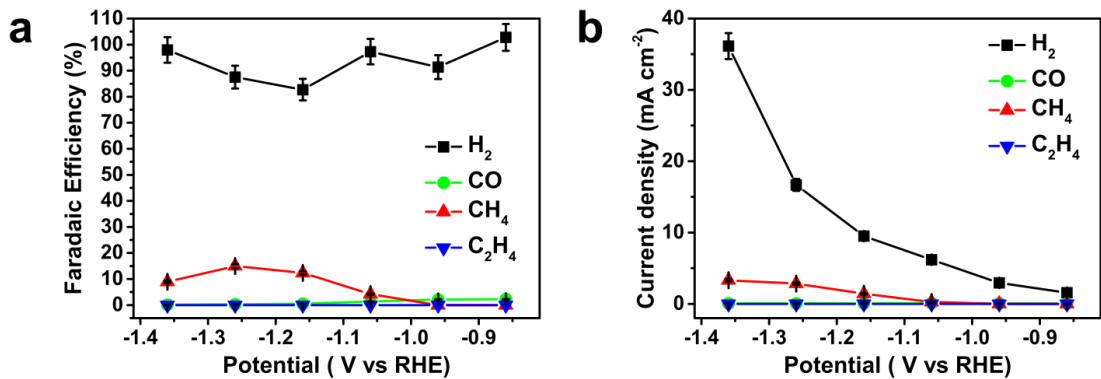
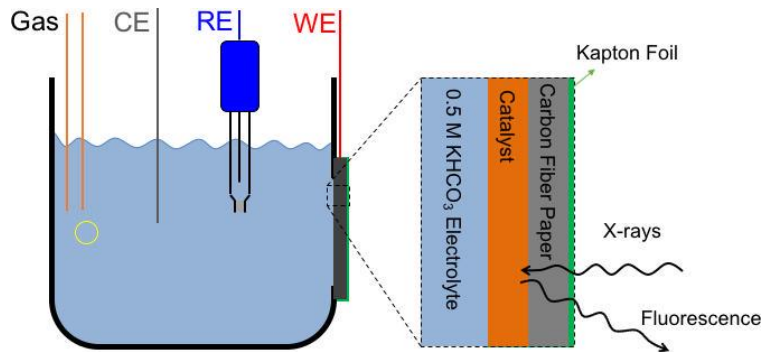


Supplementary Figure 1 | Electrocatalytic performance of HKUST-1 for CO_2 reduction. Potential-dependent **a** Faradaic efficiencies and **b** partial current densities of gas products.

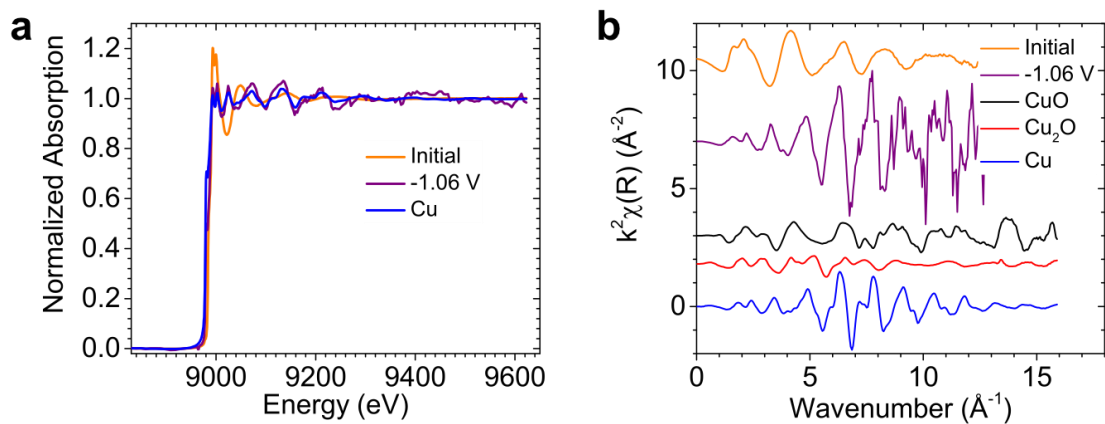


Supplementary Figure 2 | Electrocatalytic performance of $[\text{Cu}(\text{cyclam})]\text{Cl}_2$ for CO_2 reduction.

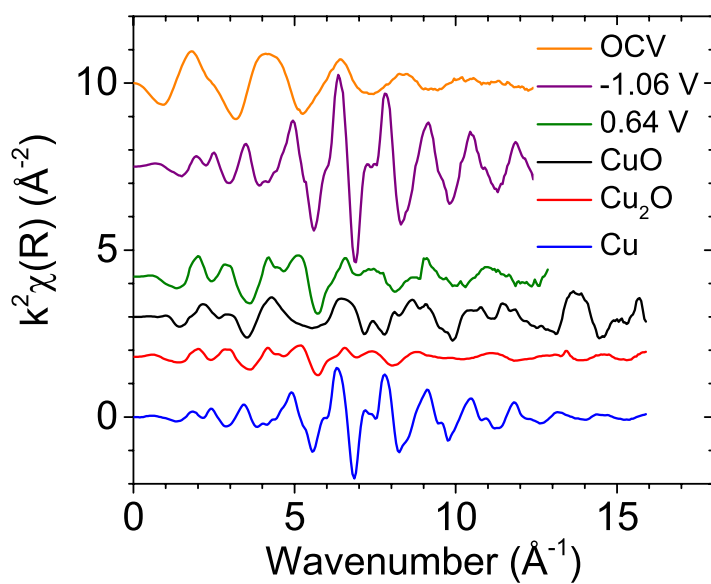
Potential-dependent **a** Faradaic efficiencies and **b** partial current densities of gas products.



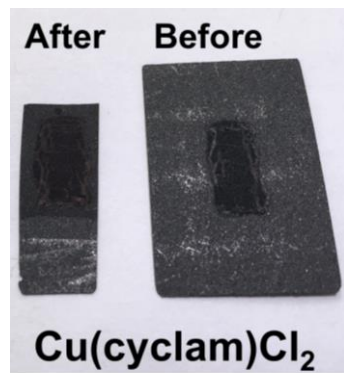
Supplementary Figure 3 | Schematic structure of the electrochemical cell used for *in-situ* XAS setup experiments. The catalyst material was deposited on the front side of the carbon fiber paper in contact with the CO₂-saturated 0.5 M KHCO₃ aqueous electrolyte. Kapton foil was applied on the back side of the carbon fiber paper facing the incident X-ray to avoid air entering the cell. CE, RE, and WE stand for counter, reference and working electrodes, respectively.



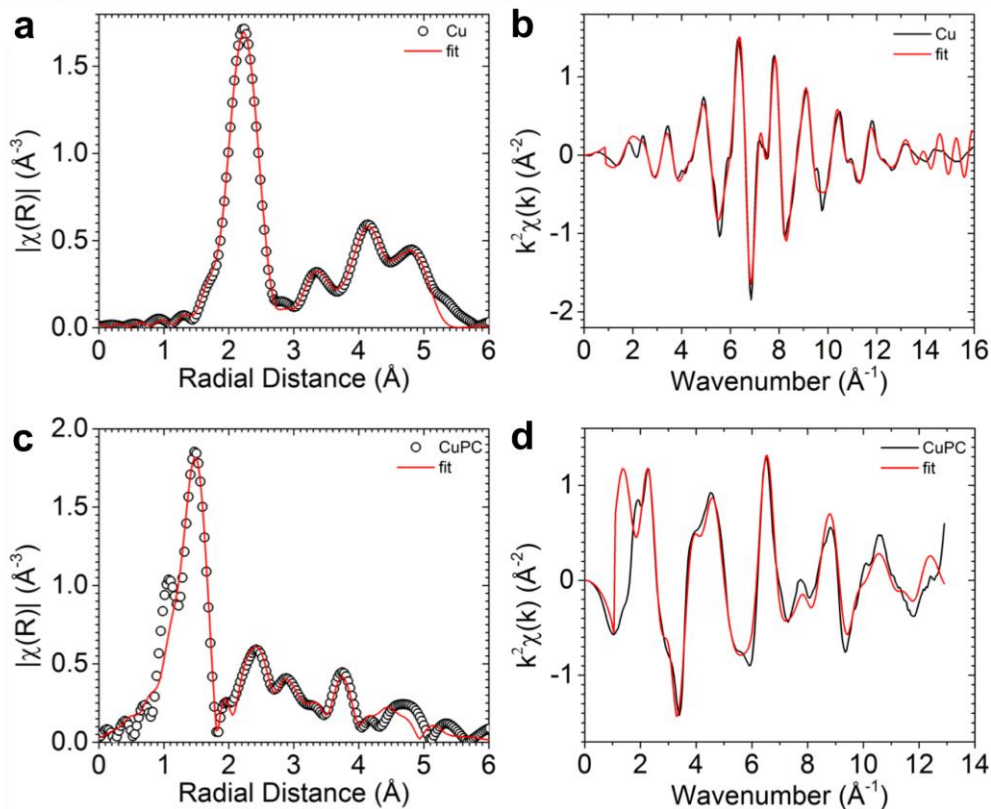
Supplementary Figure 4 | *In-situ* XAS measurements of $[\text{Cu}(\text{cyclam})]\text{Cl}_2$ under electrochemical CO_2 reduction conditions. a XAS and **b** k-space EXAFS spectra. Cu metal formed at -1.06 V vs RHE detached from the electrode, causing much noise in the XAS spectrum and the EXAFS plot.



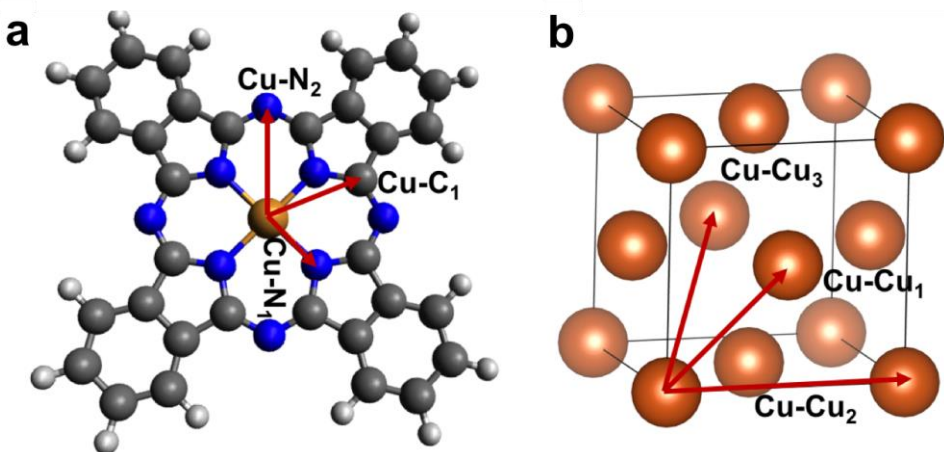
Supplementary Figure 5 | *In-situ* k-space EXAFS spectra of HKUST-1 under electrochemical CO_2 reduction conditions.



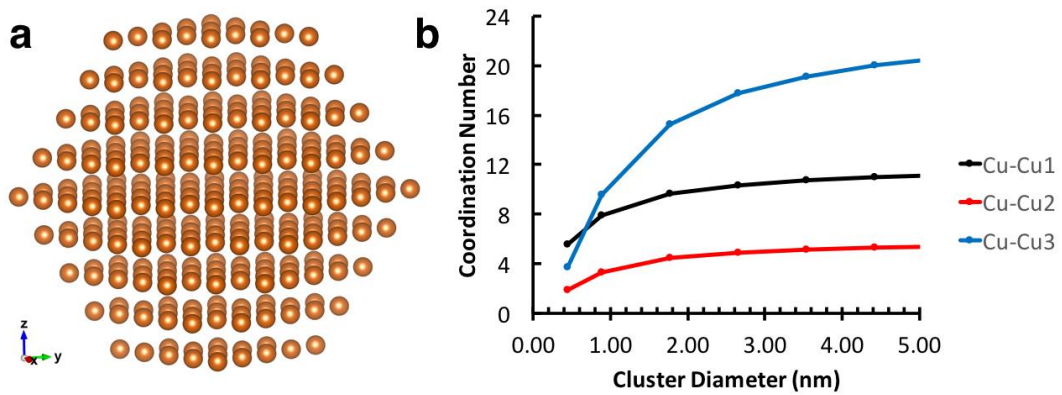
Supplementary Figure 6 | Photos of $[\text{Cu}(\text{cyclam})\text{Cl}_2]$ catalyst electrodes before and after electrocatalysis.



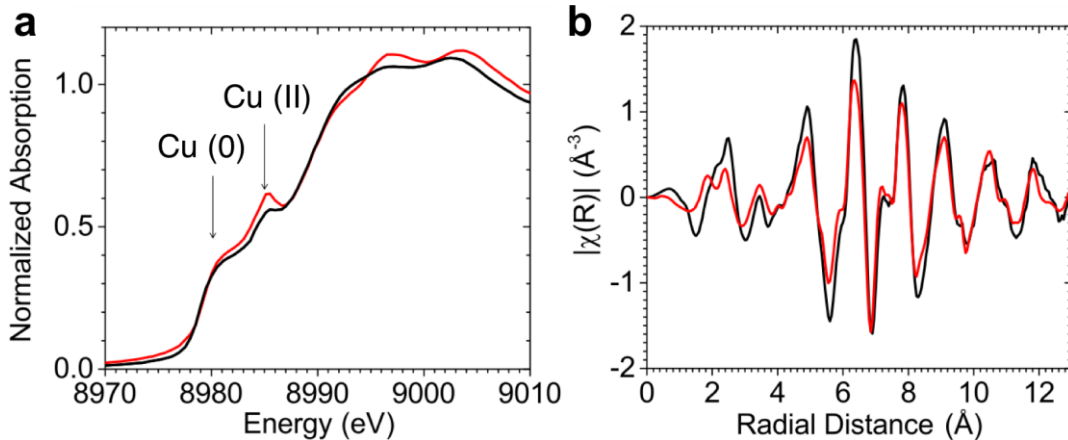
Supplementary Figure 7 | EXAFS fits for standards. **a** Cu metal R-space, **b** Cu metal k-space, **c** CuPc R-space, and **d** CuPc k-space.



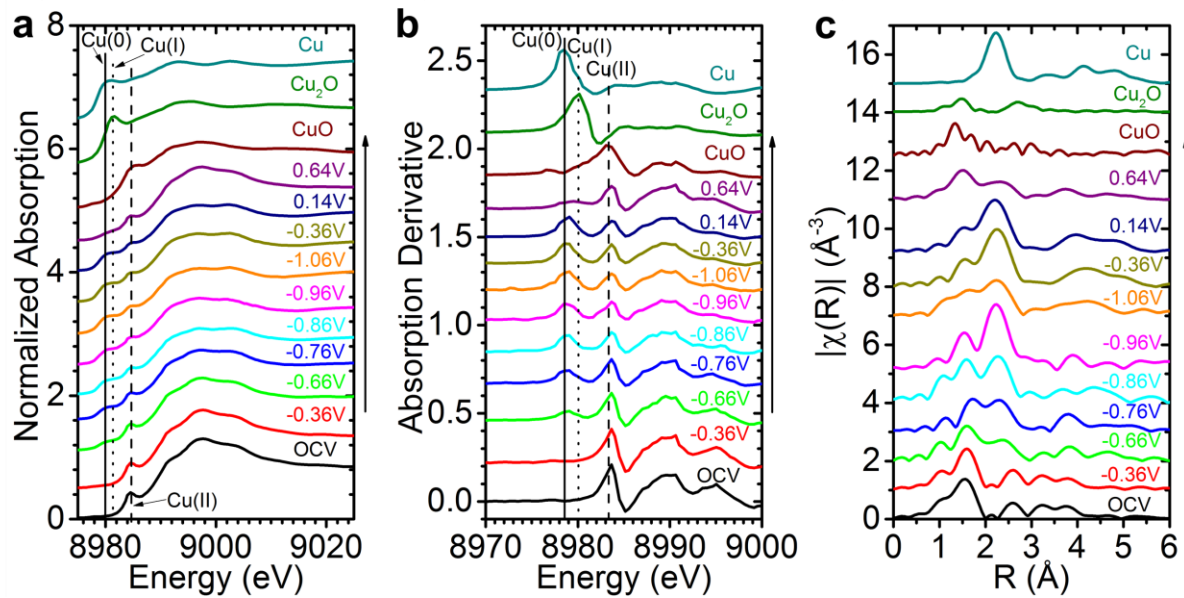
Supplementary Figure 8 | Atomic structures used for EXAFS fitting. **a** CuPc and **b** metallic Cu. The major scattering paths listed in Supplementary Table 1 are denoted here. Other scattering paths (e.g., multiple-scattering and fourth shell paths) used in fitting are not shown here. Color key: light grey - H; dark grey - C; blue - N; orange - Cu.



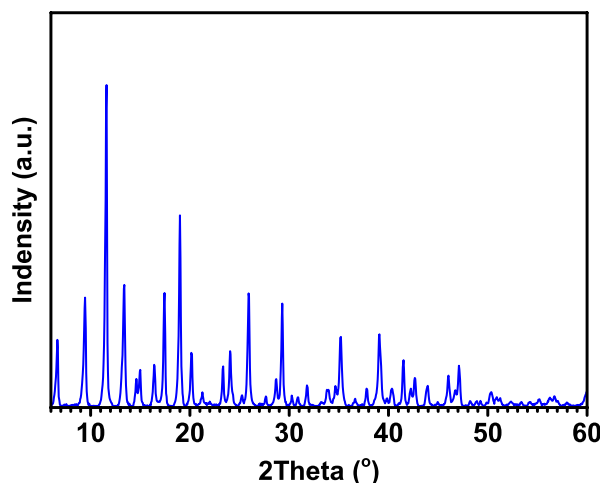
Supplementary Figure 9 | Cu nanocrystal model and its size-dependent Cu-Cu CNs for the first three shells of nearest neighbors. **a** A five-shell cuboctahedral Cu nanocrystal model. Areas shaded in blue and green represent (111)- and (100)-type planes, respectively. **b** Size-dependent Cu-Cu CNs for the first three shells of nearest neighbors for a cuboctahedral Cu nanocrystal.



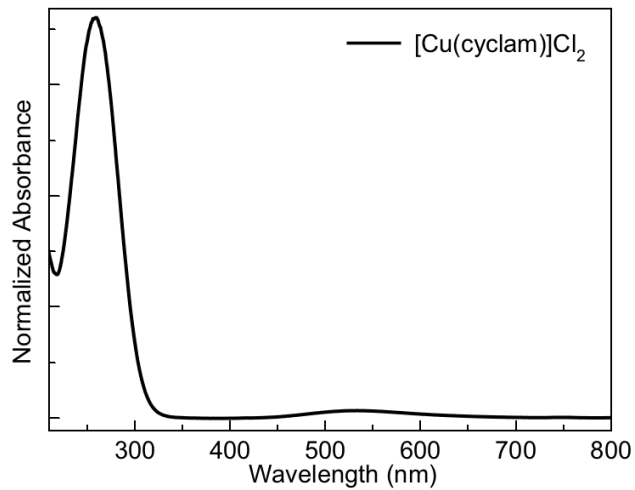
Supplementary Figure 10 | Linear combination fits of the XAS spectra of the CuPc catalyst at –1.06 V vs RHE using standard spectra of Cu foil and CuPc powder. **a** XANES and **b** EXAFS. The black lines are the measured data and the red lines are the fits.



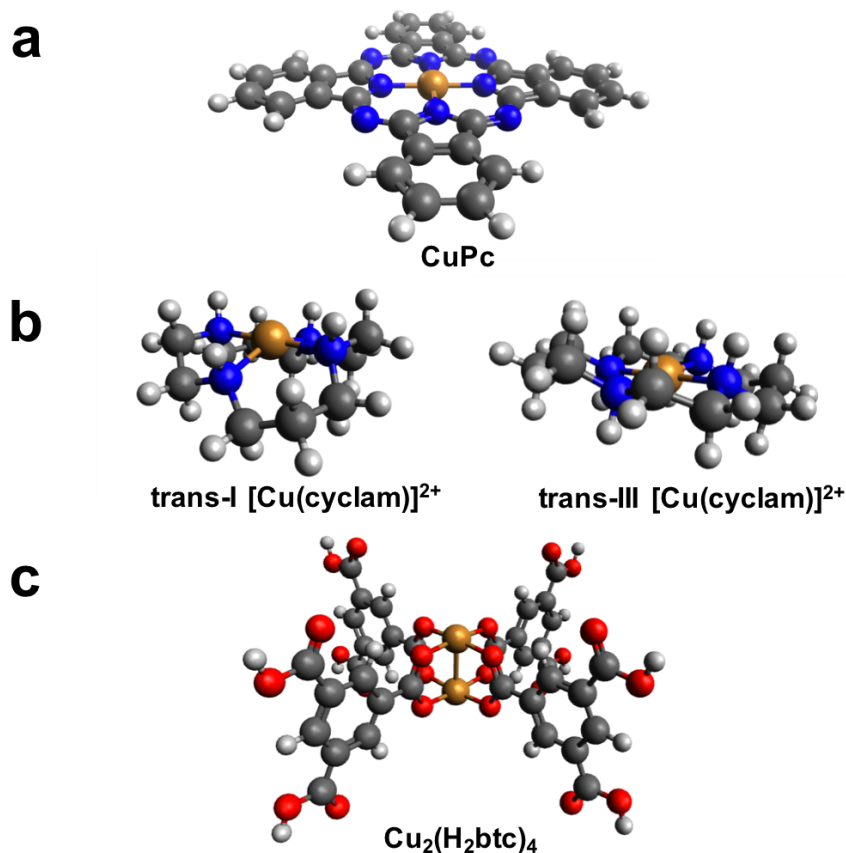
Supplementary Figure 11 | *In-situ* XAS measurements of copper(II)-5,10,15,20-tetrakis(2,6-dihydroxyphenyl)-porphyrin under electrocatalytic reaction conditions. **a** Cu K-edge XANES spectra, **b** first-order derivatives of the XANES spectra, and **c** Fourier-transformed Cu K-edge EXAFS spectra.



Supplementary Figure 12 | XRD pattern of as-synthesized HKUST-1 powder.



Supplementary Figure 13 | UV-Vis absorption spectrum of $[\text{Cu}(\text{cyclam})]\text{Cl}_2$ in CH_3OH .



Supplementary Figure 14 | DFT-optimized structures. **a** CuPc, **b** $[\text{Cu}(\text{cyclam})]^{2+}$ (trans-III and trans-I are two known isomers of metal cyclam complexes) and **c** $\text{Cu}_2(\text{H}_2\text{btc})_4$ (a dimer unit of HKUST-1). Color key: light grey - H; dark grey - C; blue - N; red - O; orange - Cu.

Supplementary Table 1 | Fitting parameters of the co-refined EXAFS spectra of CuPc at different potentials (R: distance; σ^2 : mean-square disorder; E_0 : energy shift). The single digit numbers in parentheses for R are the last digit errors. The numbers in parentheses for CN are the full errors. The scattering paths (e.g., Cu-N₁ and Cu-Cu₁) are labeled in Supplementary Figure 8.

Molecular CuPc										
	Cu-N ₁			Cu-C ₁			Cu-N ₂			
	CN	R (Å)	σ^2 (Å ²)	CN	R (Å)	σ^2 (Å ²)	CN	R (Å)	σ^2 (Å ²)	E_0 (eV)
Bulk	4	1.952	-	8	2.995	-	4	3.404	-	2.9(8)
OCV	4.0(0.5)	1.92(1)	0.005	5.2(1.3)	2.95(1)	0.002	4.0(0.5)	3.35(1)	0.011	
-0.36	3.8(0.4)	1.92(1)	0.005	5.1(0.8)	2.95(1)	0.002	3.8(0.4)	3.35(1)	0.011	
-0.66	2.1(0.3)	1.92(1)	0.005	3.5(0.8)	2.95(1)	0.002	2.1(0.3)	3.35(1)	0.011	
-0.76	1.9(0.3)	1.92(1)	0.005	3.3(0.8)	2.95(1)	0.002	1.9(0.3)	3.35(1)	0.011	
-0.86	1.6(0.3)	1.93(1)	0.005	1.8(0.9)	2.95(8)	0.002	-	-	-	
-0.96	1.3(0.4)	1.93(1)	0.005	2.4(1.1)	2.95(8)	0.002	-	-	-	
-1.06	1.2(0.5)	1.93(1)	0.005	2.6(1.5)	2.95(8)	0.002	-	-	-	
-0.36	1.2(0.5)	1.93(1)	0.005	2.6(1.5)	2.95(8)	0.002	-	-	-	
0.64	3.8(0.9)	1.92(1)	0.005	4.9(1.2)	2.95(1)	0.002	3.8(0.9)	3.35(1)	0.011	
Cu Clusters										
	Cu-Cu ₁			Cu-Cu ₂			Cu-Cu ₃			
	CN	R (Å)	σ^2 (Å ²)	CN	R (Å)	σ^2 (Å ²)	CN	R (Å)	σ^2 (Å ²)	E_0 (eV)
Bulk	12	2.556	-	6	3.615	-	24	4.427	-	3.5(9)
OCV	-	-	-	-	-	-	-	-	-	
-0.36	-	-	-	-	-	-	-	-	-	
-0.66	0.4(0.3)	2.53(1)	0.003	0.6(0.9)	3.60(3)	0.003	-	-	-	
-0.76	0.8(0.4)	2.53(1)	0.003	0.7(0.9)	3.60(3)	0.003	-	-	-	
-0.86	4.5(0.5)	2.53(1)	0.003	1.1(1.3)	3.60(3)	0.003	17.5(17.5)	4.44(1)	0.007	
-0.96	5.9(0.6)	2.53(1)	0.003	1.4(1.4)	3.60(3)	0.003	14.2(3.9)	4.44(1)	0.007	

-1.06	6.5(0.9)	2.53(1)	0.003	1.4(2.0)	3.60(3)	0.003	15.8(5.6)	4.44(1)	0.007	
-0.36	6.5(0.9)	2.53(1)	0.003	1.4(2.0)	3.60(3)	0.003	15.8(5.6)	4.44(1)	0.007	
0.64	-	-	-	-	-	-	-	-	-	

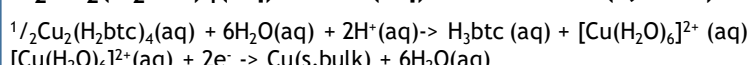
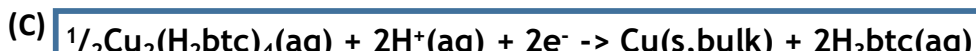
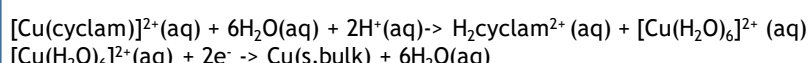
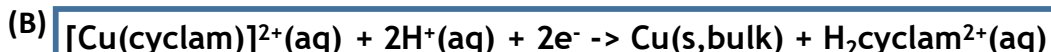
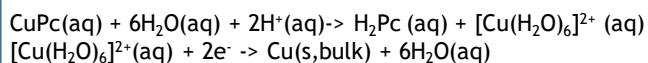
Supplementary Table 2 | Calculated size-dependent CNs of the first three nearest neighbor shells for cuboctahedral Cu nanocrystals. The CNs of Cu-Cu₁, Cu-Cu₂, and Cu-Cu₃ for bulk Cu metal are 12, 6, and 24, respectively.

Approx. Diameter (nm)	CN of Cu-Cu ₁	CN of Cu-Cu ₂	CN of Cu-Cu ₃
0.44	5.54	1.85	3.69
0.88	7.85	3.27	9.60
1.77	9.63	4.43	15.22
2.65	10.35	4.90	17.73
3.53	10.73	5.16	19.13
4.42	10.97	5.32	20.03
5.30	11.14	5.43	20.64
6.18	11.26	5.50	21.09
7.07	11.35	5.56	21.44
7.95	11.42	5.61	21.71
8.39	11.47	5.65	21.93

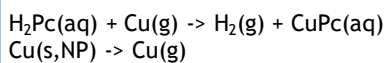
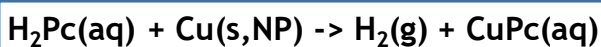
Supplementary Table 3 | Calculated free energies and standard reduction potentials of demetallation for CuPc, Cu₂(H₂btc)₄ (a dimer unit in HKUST-1), and [Cu(cyclam)]²⁺ (trans-III and trans-I are two known isomers of metal cyclam complexes).

Species	ΔG° (kcal/mol)	E° _{CuL/Cu} (V vs SHE)
CuPc	52.7	-0.80
HKUST-1	27.9	-0.27
trans-III [Cu(cyclam)] ²⁺	41.7	-0.57
trans-I [Cu(cyclam)] ²⁺	36.2	-0.45

Supplementary Note 1 | Constructed thermodynamic pathways for reductive demetallation of: (A) CuPc, (B) $[\text{Cu}(\text{cyclam})]^{2+}$ and (C) $\text{Cu}_2(\text{H}_2\text{btc})_4$ (a dimer unit in HKUST-1).



Supplementary Note 2 | Constructed thermodynamic pathway for re-metallation of H_2Pc .



Supplementary Note 3 | Synthetic route for $[\text{Cu}(\text{cyclam})]\text{Cl}_2$.

